

A Comparison of Transparent Boundary Conditions for the Fresnel Equation

David Yevick,* Tilmann Friese,* and Frank Schmidt†

*Department of Physics, University of Waterloo, Waterloo, Ontario N2L 3G1, Canada; and

†Konrad-Zuse Zentrum für Informationstechnik, Berlin, Takustr. 7,
D-14195 Berlin, Germany

Received March 6, 2000; revised August 9, 2000

We consider two numerical transparent boundary conditions that have been previously introduced in the literature. The first condition (BPP) was proposed by Baskakov and Popov (1991, *Wave Motion* **14**, 121–128) and Papadakis *et al.* (1992, *J. Acoust. Soc. Am.* **92**, 2030–2038) while the second (SDY) is that of Schmidt and Deuffhard (1995, *Comput. Math. Appl.* **29**, 53–76) and Schmidt and Yevick (1997, *J. Comput. Phys.* **134**, 96–107). The latter procedure is explicitly tailored to the form of the underlying numerical propagation scheme and is therefore unconditionally stable and highly precise. Here we present a new derivation of the SDY approach. As a result of this analysis, we obtain a simple modification of the BPP method that guarantees accuracy and stability for long propagation step lengths. © 2001 Academic Press

INTRODUCTION

Below we examine two transparent boundary conditions. The first, termed the SDY condition in the abstract, is exact and unconditionally stable. However, for the simplified version discussed in this paper, this is only true in the limit of zero transverse grid point spacing. In contrast, the second BPP condition is divergent for certain ranges of transverse and longitudinal step sizes. Here we derive a slightly modified version of the SDY formalism that generates new values for the central coefficients of the BPP method given by Eq. (26) and Eq. (27) below. Our values map the BPP method onto the SDY procedure and can be immediately employed to ensure the accuracy and stability of any BPP implementation for large longitudinal steps.

Although the SDY and BPP boundary conditions have been developed for numerous parabolic differential equations, for simplicity we specialize in the optical analog of the quantum-mechanical Schrödinger equation, namely the paraxial Fresnel equation,

$$\partial_z v = \frac{i}{2k_0 n_0} (\partial_x^2 + k_0^2 (n^2 - n_0^2)) v \quad (1)$$

for a waveguide located in the region $0 < z < Z$ with a longitudinal axis along the z -direction and a given specified initial condition $v(0)$. For a forward-propagating electric field E and an $e^{-i\omega t}$ time-dependence, $v = e^{-ik_0 n_0 z} E$ is the slowly varying component of the electric field. Here $k_0 = 2\pi/\lambda_0$, where λ_0 and n_0 are the vacuum wavelength and a suitably defined reference refractive index, respectively.

The goal of numerical boundary conditions is to supply a procedure such that the function v calculated in the internal domain of the computational window $\{x|x_- < x < x_+\}$ over the extent of the waveguide is the same as if computed on the infinite physical domain. For simplicity, since the derivation of these conditions is the same for x_- and x_+ , we examine only a right boundary point $x_+ = 0$ below and further set $n = n_0$ in the exterior domain $\{x|x \leq x_- \cup x \geq x_+\}$, where v therefore satisfies

$$\partial_z v = \frac{i}{2k_0 n_0} \partial_x^2 v. \quad (2)$$

Nonlocal (transparent) boundary conditions transform the outgoing property of waves in the external domain into a relation between the boundary value of the field at a given longitudinal position and the boundary values at all preceding propagation steps. Two methods for generating such conditions have been proposed previously. The first, introduced by Baskakov, Popov, and Papadakis (BPP), is derived by Fourier transforming the paraxial or wide-angle equation with respect to the longitudinal propagation variable [1–7]. The outgoing wave condition then maps at each boundary point to a simple algebraic relation between the longitudinal derivative of each Fourier component of the field and the field value. Inverse Fourier transforming this relation yields the boundary field values $v(x_{\pm}, z)$ at a given longitudinal distance as an integral over all previous z -values of $\partial_x v(x_{\pm}, z)$ along the boundary. However, the integral must subsequently be approximated by a discrete sum over the computed field values. While no general error analysis exists for this step, the method has been found to be conditionally stable with no minimum step size that guarantees stability in the particular case of a Crank–Nicholson longitudinal and a uniform transverse discretization with a forward (implicit) rectangular rule applied to the integral expression [7, 8]. Recently, the BPP formalism has been recast into a new, highly modified form that is exact and unconditionally stable. However, both the derivation and the numerical implementation of the resulting formulas are extremely involved and accordingly will not be considered further here [9–11].

A second, easily programmed nonlocal boundary condition was proposed in 1995 by Schmidt and Deuffhard and extended in 1999 by Schmidt and Yevick (SDY) [12–15]. Unlike the standard BPP method, which is stable only if certain numerical procedures for approximating the integral over prior field values are employed [10, 11], the SDY condition has been proved to be unconditionally stable [12]. Further, the SDY procedure fully incorporates the discrete nature of the propagation method. Note however that the procedures that we generate below are only arbitrarily accurate and unconditionally stable in the limit of zero transverse grid point spacing, as to derive corresponding formulas that are exact for arbitrary grid point spacing requires the straightforward but more lengthy treatment of [15].

To obtain a heuristic derivation but useful derivation of the SDY procedure within the framework of the Crank–Nicholson method (rigorous proofs of our assertions for an entire family of analogous second-order accurate implicit propagation procedures are presented

in [15]), we first introduce the displacement or shift operator

$$s = e^{\Delta z \frac{\partial}{\partial z}}, \tag{3}$$

with the property that $s E_{m+1} = E_m$, where Δz is the longitudinal step size, E_m denotes $E(x_b, z_m)$, and z_m is the longitudinal position at the end of m propagation steps [13]. Specializing to the Crank–Nicholson method

$$2ik_0n_0 \frac{E_{m+1} - E_m}{\Delta z} = \frac{\partial^2}{\partial x^2} \left(\frac{E_{m+1} + E_m}{2} \right) \tag{4}$$

we find immediately that

$$\frac{\partial^2 E_{m+1}}{\partial x^2} = \lambda^2 \frac{1-s}{1+s} E_{m+1} \tag{5}$$

in which $\lambda = 4ik_0n_0/\Delta z$. Defining the square root such that

$$\text{Re} \left(i \left[\frac{1-s}{1+s} \right] \right)^{1/2} \geq 0$$

for $s \in \mathbf{C}$ and setting $\lambda = \sqrt{\lambda^2}$ with $\text{Re } \lambda \geq 0$, all Fourier components of the propagating field are bounded as $x \rightarrow +\infty$ if we choose the solution

$$\frac{\partial E_{m+1}}{\partial x} = -\lambda \sqrt{\frac{1-s}{1+s}} E_{m+1} \tag{6}$$

as is justified mathematically in [15]. The square-root expression $\sqrt{\frac{1-s}{1+s}}$ is then expanded as a Taylor series in s after which the relationship $s^j E_{m+1} = E_{m+1-j}$ yields the required boundary condition for $\frac{\partial E_{m+1}}{\partial x}$ in terms of the present and past boundary values $E_{m+1}, E_m, E_{m-1} \dots E_1$.

We next establish the relationship between the BPP and SDY approaches. This requires that the SDY procedure be reformulated along the lines of the following derivation of the BPP nonlocal boundary condition [1].

BASAKOV–POPOV–PAPADAKIS (BPP) FORMULATION

To generate the BPP condition, the paraxial equation is initially Fourier transformed with respect to the longitudinal z -coordinate. The Fourier coefficients

$$c(x, k) = \int_{-\infty}^{\infty} v(x, z) e^{-ikz} dz \tag{7}$$

satisfy

$$\partial_x^2 c(x, k) = 2k_0n_0k c(x, k) \tag{8}$$

so that

$$c(x, k) = A(k)e^{\sqrt{2k_0n_0k}x} + B(k)e^{-\sqrt{2k_0n_0k}x}. \tag{9}$$

The appropriate boundary condition is $A(k) = 0$ [16] which yields

$$\sqrt{2k_0 n_0 k} c(x_+, k) + \partial_x c(x_+, k) = 0. \quad (10)$$

After inverse Fourier transforming we obtain

$$v(x_+, z) = \frac{1}{2\pi} \int_{-\infty}^{\infty} c(0, k) e^{ikz} dk = -\frac{1}{2\pi} \sqrt{\frac{i}{2k_0 n_0}} \int_{-\infty}^{\infty} \frac{1}{\sqrt{ik}} \partial_x c(x_+, k) e^{ikz} dk. \quad (11)$$

Substituting

$$\frac{1}{\sqrt{ik}} = \frac{1}{\sqrt{\pi}} \int_0^{\infty} \zeta^{-\frac{1}{2}} e^{-ik\zeta} d\zeta$$

leads to the desired Neumann-to-Dirichlet boundary condition,

$$v(x_+, z) = -(1+i) \frac{1}{\sqrt{4\pi k_0 n_0}} \int_0^{\infty} \zeta^{-\frac{1}{2}} \partial_x v(x_+, z - \zeta) d\zeta \quad (12)$$

While Eq. (12) expresses the electric field at a given boundary point in terms of the history of its transverse derivatives at the boundary, the expression is in the form of a continuous integral while numerical propagation procedures determine the electric field only at a discrete set of grid points. Accordingly, the integral must be approximated by an expression of the form

$$v(x_+, z) = -(1+i) \frac{1}{\sqrt{4\pi k_0 n_0}} \sum_{j=0}^{\infty} \alpha_j \partial_x v(x_+, z - j\Delta z). \quad (13)$$

In this paper, three standard choices for the parameter set α_j will be analyzed [17]. The first of these corresponds to associating the value of v at $z_0 + j\Delta z$ with the integral

$$\int_{z_0 + j\Delta z}^{z_0 + (j+1)\Delta z} \frac{1}{\sqrt{k}} dk \quad (14)$$

in the forward direction to yield (rectangular rule 1)

$$\alpha_j = 2\sqrt{\Delta z} \left((j+1)^{\frac{1}{2}} - j^{\frac{1}{2}} \right), \quad \alpha_0 = 2\sqrt{\Delta z}, \quad (15)$$

or alternatively

$$\alpha_j = \frac{2\sqrt{\Delta z}}{(j+1)^{\frac{1}{2}} + j^{\frac{1}{2}}}, \quad \alpha_0 = 2\sqrt{\Delta z}. \quad (16)$$

If we instead employ an integral in the reverse direction, we obtain (rectangular rule 2)

$$\alpha_j = 2\sqrt{\Delta z} \left(j^{\frac{1}{2}} - (j-1)^{\frac{1}{2}} \right) = \frac{2\sqrt{\Delta z}}{j^{\frac{1}{2}} + (j-1)^{\frac{1}{2}}}, \quad \alpha_0 = 0, \quad (17)$$

which we will later demonstrate is best suited to an implicit numerical propagation method. The BPP coefficients that will similarly be found to be best adapted to the Crank–Nicholson

procedure are derived by applying a trapezoidal integration rule to the interval between $z + (j - 1)\Delta z$ and $z + (j + 1)\Delta z$. This yields (trapezoidal rule)

$$\alpha_j = \frac{4}{3}\sqrt{\Delta z} \left((j + 1)^{\frac{3}{2}} - 2j^{\frac{3}{2}} + (j - 1)^{\frac{3}{2}} \right), \quad \alpha_0 = \frac{4}{3}\sqrt{\Delta z} \quad (18)$$

or

$$\alpha_j = \frac{4}{3}\sqrt{\Delta z} \left[\frac{3j^2 + 3j + 1}{(j + 1)^{\frac{3}{2}} + j^{\frac{3}{2}}} + \frac{-3j^2 + 3j - 1}{(j - 1)^{\frac{3}{2}} + j^{\frac{3}{2}}} \right], \quad \alpha_0 = \frac{4}{3}\sqrt{\Delta z}. \quad (19)$$

Unlike the SDY method below, the stability of the above procedure is only guaranteed for certain ranges of parameter values which necessarily depend on the integration method [7, 10, 11].

SCHMIDT-DEUFLHARD-YEVICK (SDY) FORMULATION

We now proceed to establish the connection between the BPP and SDY formalisms by deriving a slightly modified version of the SDY procedure. Our analysis proceeds as in the derivation of the BPP method above with the difference that the discrete nature of the propagation algorithm is incorporated from the beginning. In this manner we obtain a new set of the α_j coefficients that correct the accuracy and stability problems inherent in the standard BPP procedure.

To commence, we express the electric field as a Fourier series over the set of discrete longitudinal points $z_0 + j\Delta z$ rather than as a Fourier integral over z , i.e., we write

$$c_k(x) = \frac{1}{T} \int_{-\frac{T}{2}}^{\frac{T}{2}} v(x, z) e^{-2\pi i k z / T} dz. \quad (20)$$

The size of the interval T over which the Fourier series is taken is arbitrary; however, we will apply our final results in the $T \rightarrow \infty$ limit (identical results can be derived for the $z > 0$ half-space). Next, we must write an equation that specializes to the Crank–Nicholson formulation. To do this, we insert Eq. (20) into Eq. (4). This yields for the Fourier coefficients $v_k(x)$,

$$\partial_x^2 c_k(x) = \frac{4k_0 n_0}{i\Delta z} \frac{e^{2\pi i k \Delta z / T} - 1}{e^{2\pi i k \Delta z / T} + 1} c_k(x) = \frac{4k_0 n_0}{\Delta z} \tan\left(\frac{\pi k \Delta z}{T}\right) c_k(x). \quad (21)$$

The general solution for $c_k(x)$ is

$$c_k(x) = A_k e^{\sqrt{\frac{4k_0 n_0}{\Delta z} \tan\left(\frac{\pi k \Delta z}{T}\right)} x} + B_k e^{-\sqrt{\frac{4k_0 n_0}{\Delta z} \tan\left(\frac{\pi k \Delta z}{T}\right)} x}. \quad (22)$$

Thus, in analogy with Eq. (10), to ensure that the field properly decays in the right external region (the case of nonzero reflection at the boundary is described in Appendix A) we must impose $A_k = 0$ so that

$$\sqrt{\frac{4k_0 n_0}{\Delta z} \tan\left(\frac{\pi k \Delta z}{T}\right)} c_k(x_+) + \partial_x c_k(x_+) = 0. \quad (23)$$

We convert the above property of the Fourier coefficients to a boundary condition on the electric field by inverse discrete Fourier transforming as

$$v(x_+, z) = \sum_{k=-\infty}^{\infty} c_k(x_+) e^{2\pi i k z/T} = -\sqrt{\frac{i \Delta z}{4 k_0 n_0}} \sum_{k=-\infty}^{\infty} \frac{1}{\sqrt{i \tan\left(\frac{\pi k \Delta z}{T}\right)}} \partial_x c_k(x_+) e^{2\pi i k z/T}, \tag{24}$$

where the square root is defined as in Eq. (6). To evaluate this expression, we expand in powers of $e^{-2\pi i k \Delta z/T}$ according to

$$\frac{1}{\sqrt{i \tan\left(\frac{\pi k \Delta z}{T}\right)}} = \sum_{j=0}^{\infty} \beta_j e^{-2\pi i j k \Delta z/T}. \tag{25}$$

After subsequently summing over the index k , we obtain the semi-discrete boundary condition (note that the transverse derivative is still assumed continuous)

$$v(x_+, z) = -(1 + i) \sqrt{\frac{\Delta z}{8 k_0 n_0}} \sum_{j=0}^{\infty} \beta_j \partial_x v(x_+, z - j \Delta z) \tag{26}$$

where

$$\beta_j = \left(1, 1, \frac{1}{2}, \frac{1}{2}, \frac{1 \cdot 3}{2 \cdot 4}, \frac{1 \cdot 3}{2 \cdot 4}, \frac{1 \cdot 3 \cdot 5}{2 \cdot 4 \cdot 6}, \frac{1 \cdot 3 \cdot 5}{2 \cdot 4 \cdot 6}, \dots\right). \tag{27}$$

This is our main result. Specifically, Eq. (27) is the exact analog of the main BPP formula, Eq. (12), yielding BPP coefficients that are precisely matched to the Crank–Nicholson method (coefficients for related implicit and explicit numerical propagation procedures can be derived in an analogous fashion). Hence any BPP propagation code will acquire the accuracy of the SDY approach if the standard BPP coefficients Eqs. (15)–(19) are simply replaced by those of Eq. (27). The resulting program is then unconditionally stable in the limit of small transverse grid point spacing as proven in [12].

A few additional aspects of Eq. (27) should be mentioned. First, although the above expression has been derived on the half-space $z \geq 0$, it is still exact if the electric field and its first derivative are zero at the computational window boundaries for $z = 0$. Secondly, as we have mentioned earlier, the above analysis strictly applies only in the limit of zero transverse grid point spacing. To generate a precise version of the SDY procedure for finite Δx requires the introduction of an additional shift operator that relates two adjacent transverse electric field values as in [15]. Finally, note that the β_j are the absolute values of the coefficients that result from the Taylor series expansion of Eq. (6) and are in fact those obtained by solving for v in terms of $\partial_z v$ in Eq. (6) prior to expanding in powers of s . In a similar fashion, Eq. (12) can be reformulated to express $\partial_z v$ in terms of v ; however, the resulting integral formulas are, in this case, far more cumbersome (cf. Appendix B).

NUMERICAL VERIFICATION

In the preceding discussion, we developed a slightly modified version of the SDY method. This method is functionally identical to the standard BPP formalism but with a new, exact set of coefficients that guarantees stability for large longitudinal step lengths. To illustrate the practical importance of these results, we first compare the exact and approximate BPP coefficients. We then demonstrate the accuracy of the new SDY technique through a standard numerical error analysis and finally demonstrate in a benchmark computational acoustics calculation that this method, unlike the original BPP procedure, is convergent for large longitudinal step lengths.

A direct comparison of the BPP and modified SDY coefficients is presented in Fig. 1, which displays the normalized coefficients, resulting from Eq. (15) (dashed), Eq. (17) (dashed-dotted), and Eq. (18) (dotted) together with the corresponding coefficients for the modified SDY formulation for the Crank–Nicholson (solid line) and implicit (thick solid line) propagation methods, given by the Taylor series coefficients of $\frac{\sqrt{\pi}}{2} \left(\frac{1+s}{1-s}\right)^{1/2}$ and $\frac{\sqrt{\pi}}{2} (1-s)^{-1/2}$ (cf. Eq. 26). Clearly, the BPP trapezoidal rule coefficients are closest to the exact Crank–Nicholson coefficients while applying the rectangular rule 2 (backward integration formula) for the BPP integral instead leads to an acceptable approximation to the exact implicit method coefficients. In each case, however, the BPP values diverge noticeably from the SDY results especially at small j .

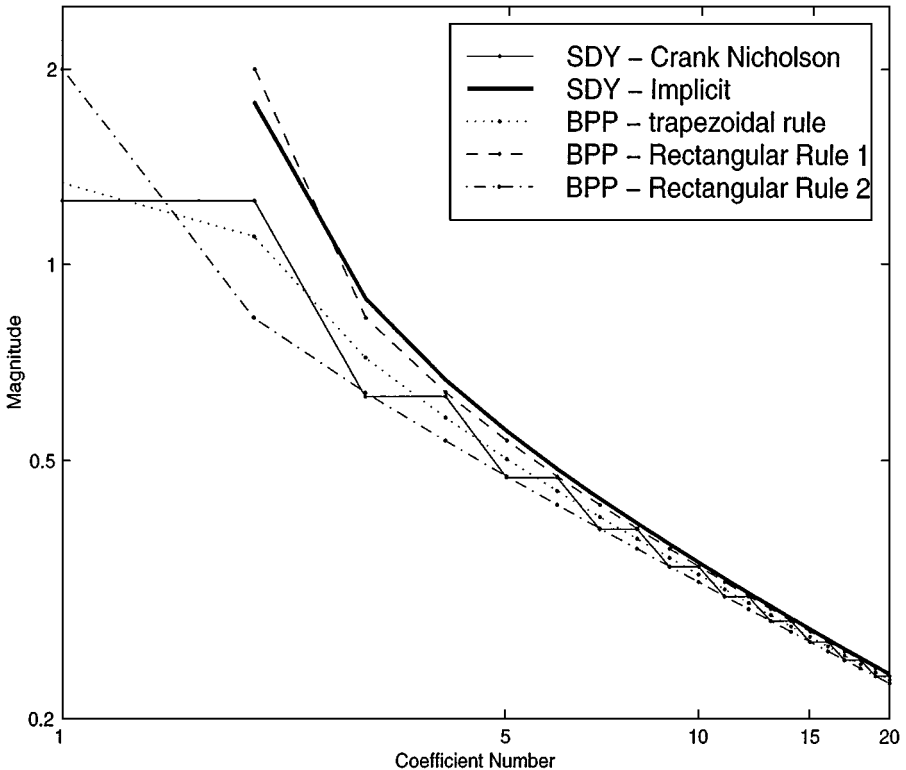


FIG. 1. The coefficients for the BPP backward rectangular integration formula (dashed), the BPP forward integration formula (dashed-dotted), the BPP trapezoidal integration formula (dotted), the modified SDY Crank–Nicholson method (solid line), and the modified SDY implicit method (thick solid line).

Next, we present a numerical error analysis of the modified SDY procedure, Eq. (26), by considering the reflection of a Gaussian beam described by

$$E(x, 0) = e^{-x^2/100} e^{-k_0 n_0 \sin(\pi/9)x} \quad (28)$$

from the computational window boundary as a function of the number of transverse grid points. In the calculation, the computational window width is $150 \mu\text{m}$, $n = n_0 = 1$, the longitudinal step size $\Delta z = 0.4 \mu\text{m}$, and the vacuum light wavelength $\lambda = 1.55 \mu\text{m}$. When we examine Fig. 2, which displays the power remaining in the computational window as a function of propagation distance and number of transverse grid points, N , we observe that the reflection induced by the transparent boundary condition decreases as the square of the grid point spacing. This behavior, which is entirely analogous to that of Fig. 5 in Ref. [13], arises from the second-order nature of the finite-element method applied to implement the continuous derivative appearing in the modified SDY boundary condition. In applying transparent boundary condition to the Crank–Nicholson method, Eq. (4), we have written, e.g., for the right-hand boundary

$$\frac{\partial^2 v}{\partial x^2}(x_+, z) \approx \frac{2}{(\Delta z)^2} \left(v(x_+ - \Delta x, z) - v(x_+, z) + \Delta x \frac{\partial v}{\partial x}(x_+, z) \right) \quad (29)$$

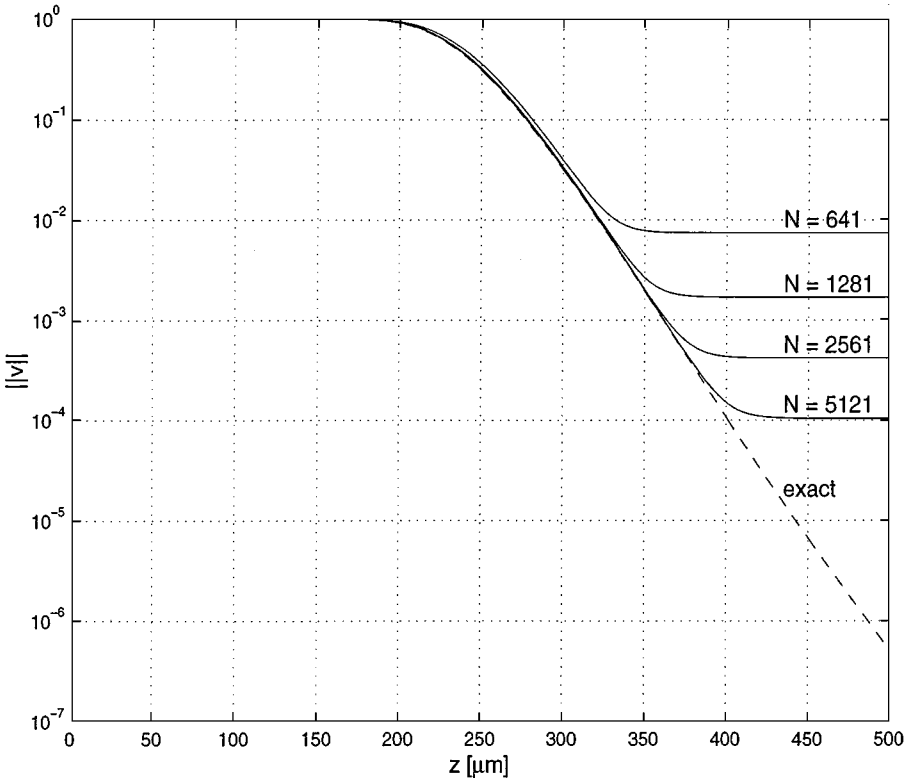


FIG. 2. The power remaining in the computational window for a Gaussian beam impinging on the computational window boundary for the modified SDY method as a function of propagation distance and number of transverse grid points.

and

$$\frac{\partial^2 v}{\partial x^2}(x_+ - \Delta x, z) \approx \frac{1}{4(\Delta z)^2} \left(v(x_+ - 3\Delta x, z) - v(x_+ - \Delta x, z) + 2\Delta x \frac{\partial v}{\partial x}(x_+, z) \right). \quad (30)$$

The partial derivatives appearing on the right-hand side of the above equations are then replaced by values computed by Eq. (26) or Eq. (13), and the derivative $\frac{\partial v}{\partial x}(x_+, z)$ is regarded as a separate, fictitious degree of freedom. While such a formulation is non-Hermitian, the imaginary part of the (three) spurious eigenvalues associated with the Crank–Nicholson propagation matrix vanish in the limit of zero grid point spacing. An alternative procedure is to replace $\frac{\partial v}{\partial x}(x_+, z)$ in Eq. (26) or Eq. (13) by $v(x_+ + \Delta x, z) - v(x_+, z)$ and then to consider $v(x_+ + \Delta x, z)$ as the additional degree of freedom.

Finally, we demonstrate that the modified SDY method is convergent for large longitudinal step lengths in contrast to the standard BPP method. To relate our calculation to previous literature, we revisit the standard benchmark underwater acoustic test case employed by M. Mayfield in [7] to prove the lack of stability of the BPP method. However, we consider the case of small transverse and long longitudinal step lengths. In this limit, divergences arising from the approximate treatment of the transverse problem employed for both the SDY and BPP methods in this paper are suppressed while the unconditional longitudinal stability afforded by the modified SDY method becomes apparent. We again employ the paraxial wave equation (Tappert PE) in our example.

Hence we consider an ocean 100 m in depth with a sound velocity of 1500 m/s and a density of 100 g/cm³ above a lossless bottom layer with a sound velocity of 1550 m/s and density of 1.2 g/cm³. A 500 Hz point source is located at an ocean depth of 50 m; the change in acoustic pressure is then recorded at the same 50 m depth at ranges of up to 100 m. In contrast to [7], in which a transverse (depth) step of 5 m and a 20 point transverse grid was selected, we employ a 1 m transverse grid point spacing and 200 transverse grid points to ensure that any instabilities arise from errors in the numerical description of the problem in the longitudinal direction and not from the lack of high-order accuracy in the evaluation of transverse derivatives, which is shared by both approaches in our present treatment. The propagation loss curves, as a function of longitudinal distance (range) for a large 100 m longitudinal step length for both the modified SDY (solid line), and standard BPP formalism (dashed line), are presented in Fig. 3. While the two sets of results nearly agree at small ranges, the error and numerical instability of the original BPP formalism are apparent for ranges beyond 2 km, clearly proving the assertions of this paper.

CONCLUSIONS

While the BPP formalism previously has been the preferred method for implementing transparent boundary conditions in two-dimensional paraxial propagation problems, we have demonstrated in this paper that the unconditionally stable SDY procedure has the same theoretical justification as the BPP method yet is intrinsically more accurate and simpler to implement. Our theoretical development has also established the intrinsic error of the BPP formulation and has provided a correspondence between different methods of approximating the continuous BPP result and discrete numerical propagation schemes. In the context of two companion papers which extend the SDY formalism to wide-angle

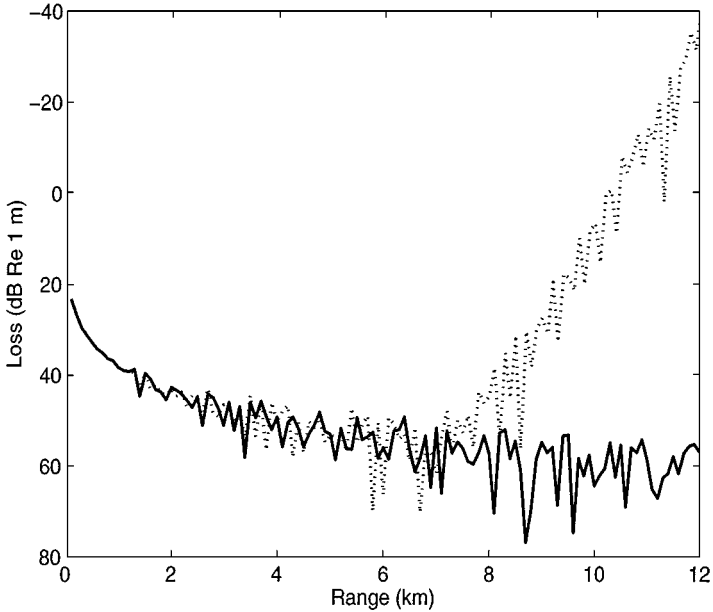


FIG. 3. The propagation loss versus range for the acoustic test case of [7] as computed with the modified SDY (solid line) and the standard BPP (dashed line) formalisms.

propagation algorithms [18–20], the results of this article clearly establish the practical and theoretical importance of future generalizations of the SDY procedure.

APPENDIX A: CONTINUOUS VERSION OF SDY METHOD

The BPP formalism can be easily modified to yield a Dirichlet-to-Neumann boundary condition that is the analog of the standard SDY formula, Eq. (6). The boundary condition that results in place of Eq. (12), namely,

$$\partial_x v(x_+, z) = (1 - i) \sqrt{\frac{n_0 k_0}{\pi}} \left(\frac{1}{2} \int_0^z (z')^{-3/2} v(x_+, z - z') dz' - \lim_{z' \rightarrow 0} \sqrt{z'} v(x_+, z - z') \right) \quad (31)$$

can be obtained either directly from the half-space Fourier transform of the square root appearing in Eq. (10) or by inverting Eq. (12) with respect to the Neumann data using the Abel inversion formula. In the latter case, one obtains the intermediate expression

$$\partial_x v(x_+, z) = -\sqrt{\frac{2n_0 k_0}{\pi i}} \frac{d}{dz} \int_0^z (z')^{-1/2} v(x_+, z - z') dz', \quad (32)$$

which reduces to Eq. (31) after evaluating the derivative and subsequently integrating by parts. Presumably because of the numerical complications associated with evaluating Eq. (31), to our knowledge this result has not appeared previously in the literature.

APPENDIX B: INCORPORATION OF BOUNDARY REFLECTION

If the refractive index in the region external to the boundary is inhomogeneous, each Fourier component c_k will be partially reflected with an effective reflection coefficient R_k at the computational window boundary. Eq. (23) then becomes

$$\frac{1 - R_k}{1 + R_k} \sqrt{\frac{4k_0 n_0}{\Delta z} \tan\left(\frac{\pi k \Delta z}{T}\right)} c_k(x_+) + \partial_x c_k(x_+) = 0. \quad (33)$$

Expanding $(1 - R_k)/(1 + R_k)$, viewed as a function of the discrete argument k , as the Fourier series

$$\frac{1 - R_k}{1 + R_k} = \sum_{j=0}^{\infty} \xi_j e^{-i2\pi j k \Delta z / T} \quad (34)$$

we obtain after inverse Fourier transforming

$$\partial_x v(x_+, z) = -(1 - i) \sqrt{\frac{2k_0 n_0}{\Delta z}} \sum_{j=0}^{\infty} \left(\sum_{l=0}^j \alpha_{j-l} \xi_l \right) v(x_+, z - j \Delta z) \quad (35)$$

in place of Eq. (13). Obviously, the major difficulty in applying Eq. (35) is the limited number of reflection coefficients for which the inner sum has a simple analytic form [21, 22].

ACKNOWLEDGMENTS

Support for this work was provided by the Canadian Institute for Photonic Innovations, Nortel Networks, and the National Sciences and Research Council of Canada. We thank D. Thomson of DREA, who provided the benchmark propagation code employed in Fig. (3).

REFERENCES

1. V. A. Baskakov and A. V. Popov, Implementation of transparent boundaries for numerical solution of the Schrodinger equation, *Wave Motion* **14**, 121 (1991).
2. M. E. Mayfield and D. J. Thomson, An FFT-based non-local boundary condition for the parabolic equation, in *3rd European Conference on Underwater Acoustics*, edited by J. S. Papadakis (Crete Univ. Press, Heraklion, 1996), Vol. 1, pp. 237–242.
3. A. V. Popov, Accurate modeling of transparent boundaries in quasi-optics, *Radio Sci.* **31**, 1781 (1996).
4. J. S. Papadakis, Impedance formulation of the bottom boundary condition for the parabolic equation model in underwater acoustics, in J. A. Davis *et al.*, *op cit.*, p. 83.
5. M. E. Mayfield and D. J. Thomson, A non-reflecting boundary condition for use in PE calculations of sound propagation in air, *J. Acoust. Soc. Am.* **92**, 2406 (1992).
6. J. S. Papadakis, Exact, nonreflecting boundary conditions for parabolic-type approximations in underwater acoustics, *J. Comput. Acoust.* **2**, 83 (1994).
7. B. Mayfield, Nonlocal Boundary Conditions for the Schrödinger Equation, Ph.D. thesis (University of Rhode Island, Providence, RI, 1989).
8. A. Arnold, Numerically Absorbing Boundary Conditions for Quantum Evolution Equations, in *Proceedings of the International Workshop on Computational Electronics, VLSI-Design 63-5*, Tempe, AR, 1995.
9. A. Arnold, Numerically absorbing boundary conditions for quantum evolution equations, *VLSI Design* **6**(1–4), 313 (1998).

10. A. Arnold, On absorbing boundary conditions for quantum transport equations, *Math. Modell. Numer. Anal.* **28**, 853 (1994).
11. A. Arnold and M. Ehrhardt, Discrete transparent boundary conditions for wide angle parabolic equations in underwater acoustics, *J. Comput. Phys.* **145**, 611 (1998).
12. F. Schmidt and P. Deuffhard, Discrete transparent boundary condition for the numerical solution of Fresnel's equation, *Comput. Math. Appl.* **29**, 53 (1995).
13. F. Schmidt and D. Yevick, Analysis of boundary conditions for the Fresnel equation, *J. Comput. Phys.* **134**, 96 (1997).
14. D. Yevick and D. J. Thomson, Nonlocal boundary conditions for finite-difference parabolic equation solvers, *J. Acoust. Soc. Am.* **106**, 143 (1999).
15. F. Schmidt, Construction of discrete transparent boundary conditions for Schrödinger-type equation, *Surv. Math. Ind.* **9**, 87 (1999).
16. J. S. Papadakis, M. I. Taroudakis, P. J. Papadakis, and B. Mayfield, A new method for a realistic treatment of the sea bottom in the parabolic approximation, *J. Acoust. Soc. Am.* **92**, 2030 (1992).
17. D. J. Thomson and M. E. Mayfield, An exact radiation condition for use with the *a posteriori* PE method, *J. Comput. Acoust.* **2**, 113 (1994).
18. T. Friese, F. Schmidt, and D. Yevick, Transparent boundary conditions for a wide-angle approximation of the one-way Helmholtz equation, submitted for publication.
19. M. D. Collins, A split-step Padé solution for the parabolic equation method, *J. Acoust. Soc. Am.* **93**, 1736 (1993).
20. F. Schmidt, T. Friese, and D. Yevick, Transparent Boundary Conditions for Split-Step Padé Approximations of the One-Way Helmholtz equation, Preprint SC99-46 (Konrad-Zuse-Zentrum Berlin, 1999).
21. D. J. Thomson, G. H. Brooke, and E. S. Holmes, PE approximations for scattering from a rough surface, Technical Memo. 95-21 (Defense Research Establishment Pacific, Victoria, B.C., 1995).
22. G. H. Brooke, D. J. Thomson, and P. M. Wort, A sloping-boundary condition for efficient PE calculations in range-dependent acoustic media, *J. Comput. Acoust.* **4**, 11 (1996).